# Surface and bulk chemistry of chemically amplified photoresists: segregation in thin films and environmental stability issues

Erin L. Jablonski[1,*], Vivek M. Prabhu[1], Sharadha Sambasivan[1], Daniel A. Fischer[2], Eric K. Lin[1], Dario L. Goldfarb[3], Marie Angelopoulos[3], and Hiroshi Ito[4]

[1]Polymers and [2]Ceramics Divisions, National Institute of Standards and Technology
Gaithersburg, MD 20899
[3]IBM T. J. Watson Research Center, Yorktown Heights, NY 10598
[4]IBM Almaden Research Center, San Jose, CA 95120

## ABSTRACT

The performance of chemically amplified photoresists, including next generation thin film 157 nm fluorinated copolymers and blends, is affected by such phenomena as polymer/substrate and polymer/air interfacial (surface energy) effects, blend miscibility, small molecule diffusion in thin films, permeability of airborne contaminants, and interactions with products from the deprotection reaction. Using near edge x-ray absorption fine structure (NEXAFS) spectroscopy, it is possible to simultaneously probe the surface and bulk chemistry of chemically amplified photoresists to determine possible causes of pattern degradation, including post exposure delay induced material failure, blend component and small molecule diffusion/segregation to the photoresist surface, and interactions between components of the photoresist formulation and developer. The surface and bulk chemistry of model photoresists were analyzed in the NEXAFS vacuum chamber, equipped with *in situ* processing capabilities for exposure, controlled dosing of a model contaminant gas (NMP or water vapor), and heating, to quantify component segregation and identify surface phenomena that may be responsible for pattern degradation. For model 157 nm blend films, it was found that there is segregation of one component to the surface of the photoresist film, in excess of the composition of that component in the blend. For polymer blends the more hydrophobic or lower surface tension species will typically wet the film surface when heated in air. Segregation of photo-acid generator has also been demonstrated and the effect of reducing film thickness investigated. As photoresist film thickness continually decreases and the photoresists become increasingly sensitive to environmental contaminants, the interfacial and surface regions dominate the behavior of the material and it is crucial to understand both their physical and chemical nature.

**Keywords:** NEXAFS, blend miscibility, airborne molecular contaminants

## 1. INTRODUCTION

The 2003 International Technology Roadmap for Semiconductors specifies a target line width for 2004 of only 90 nm and projects sub-50 nm features and sub-200 nm film thickness by 2010.[1] Advances in optical lithography continue to meet these goals pushing the ultimate resolution of chemically amplified photoresists to molecular dimensions. As photoresist films become thinner and formulations continually change, concerns including polymer/substrate and polymer/air interfacial (surface energy) effects, miscibility, small molecule diffusion, and permeability of airborne contaminants become crucial in the overall performance of the material. These issues are magnified in ultra-thin films and multilayer systems. While the technology to create patterns for integrated circuitry progresses, techniques that are able to access surface versus bulk chemical information become instrumental in determining failure mechanisms, chemical changes, distribution of components, etc. Chemically amplified photoresists are prone to interfacial and surface chemical changes that cause deviations in the desired lithographic pattern such as T-topping and closure. For example, if interfacial excess or depletion of the photo-generated acid occurs, either from atmospheric contamination, evaporation, or segregation within the film, the resulting compositional heterogeneity will affect the interfacial photoresist structure, composition, deprotection kinetics and/or dissolution behavior during development, particularly for

---

* erin.jablonski@nist.gov

photo-acid generators that can also act as dissolution modifiers. Near edge x-ray absorption fine structure (NEXAFS) spectroscopy can probe the surface and bulk chemistry of these chemically amplified photoresists to determine possible causes of pattern degradation, including polymer component and small molecule diffusion/segregation to the photoresist surface, post exposure delay induced material failure, and interactions between components of the photoresist formulation and developer.
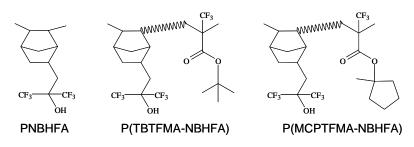
Ito et al. have proposed a formulation strategy employing blends of different potential 157 nm fluorinated homopolymers and copolymers.[2] They found that the protected copolymer could act as a dissolution inhibitor to the homopolymer to provide enhanced patterning capability. The surface and bulk chemistry of a 157 nm photoresist blend system were analyzed using NEXAFS to quantify component segregation and identify surface phenomena that may impact pattern formation. Spectral combinations of the constituent polymers are used to fit the spectra of the blend films as a function of various processing conditions. Significant segregation of one component to the surface of the photoresist film was found, in excess of the composition of that component in the blend. The bulk data were consistent with initial blend compositions. Implications for the performance of thin film photoresist blends are discussed.

Chemically amplified photoresists have been developed to limit their environmental sensitivity so that degradation of an imaged pattern does not occur during processing, particularly with respect to post-exposure delay (PED). Positive tone chemically amplified photoresists make use of a photo-generated acid and polymer with acid-labile protecting groups that are cleaved off to form an aqueous base soluble material. In order to maintain integrity of imaged patterns, the chemistry of deprotection must not be compromised by exposure to airborne molecular contaminants, especially basic contaminants that can quench the acid and inhibit deprotection. For this reason, photoresist pattern fabrication is done in filtered air with amines present at parts per billion (ppb) levels. Although contaminant effects on photoresist films have previously been investigated,[3,4] the technique discussed here allows *in situ* processing of samples in a well controlled environment followed by immediate surface analysis. The effect of the introduction of contaminant vapor during PED on photoresist performance was quantified by following the extent of deprotection at the film surface for different processing conditions.

## 2. EXPERIMENTAL[†]

**Materials and methods**

The photoresists used in the 157 nm blend films studies are poly(norbornene hexafluoroalcohol) (PNBHFA) and two random copolymers, poly(*t*-butyltrifluoromethacrylate-co-norbornene hexafluoroalcohol) (P(TBTFMA$_{0.60}$-NBHFA$_{0.40}$)) and poly(methylcyclopentyl 2-trifluoromethacrylate-co-norbornene hexafluoroalcohol) [P(MCPTFMA$_{0.58}$-NBHFA$_{0.42}$)], with the photo-acid generator (PAG) di(4-*t*-butylphenyl) iodonium perfluorooctanesulfonate (PFOS). Pure component and various blend compositions of PNBHFA:P(TBTFMA-NBHFA) and PNBHFA:P(MCPTFMA-NBHFA) were prepared as 4 %, 3 %, and 2 % mass fraction solutions in propylene glycol methyl ether acetate (PGMEA). Some films were also cast from cyclohexanone and ethyl lactate. Films were prepared from these solutions by spin-coating onto silicon wafers followed by a post apply bake (PAB) at 130 °C for 60 s. In addition, 50:50 blend films were prepared containing 5 % mass fraction PFOS from 4 %, 3 %, and 2 % mass fraction PGMEA solutions. Some films were subject to PAB only; others were exposed to ultra violet (UV) at ≈ 450 mJ/cm$^2$ and post-exposure baked (PEB) at 130 °C for 60 s. The structures of PNBHFA, P(TBTFMA-NBHFA), and P(MCPTFMA-NBHFA) are shown below.



PNBHFA          P(TBTFMA-NBHFA)          P(MCPTFMA-NBHFA)

Silicon wafers for studies of developed blend films were prepared as follows: 5 min exposure to oxygen plasma followed by removal of the native oxide layer by subsequent immersion into a solution of $(10 \pm 2)$ % volume fraction hydrofluoric acid and $(5 \pm 2)$ % volume fraction ammonium fluoride in ultra pure water for $(60 \pm 5)$ s. An oxide layer was grown in a UV/Ozone chamber for $(120 \pm 1)$ s followed by priming with hexamethyldisilazane (HMDS) vapor. Blends films (50:50 mass ratio) were spin-coated and PAB as described above. Samples were then developed by immersion into TMAH solutions for 30 s followed by immersion for 30 s into fresh deionized water with resistivity 18.0 MΩ-cm purified by a Milli-Q UF Plus system. TMAH solutions were prepared by dilution with deionized water of a stock solution (mass fraction of 10 %), purchased from Aldrich Chemicals.

For *in situ* environmental stability studies, a model photoresist system comprising poly((*t*-butoxycarbonyloxy)styrene) (PBOCSt) and the photo-acid generator (PAG) bis(*p-t*-butylphenyl) iodonium perfluorooctanesulfonate (PFOS) was chosen. Samples were prepared by spin coating films of PBOCSt with 5 % mass fraction PFOS from a 9 % mass fraction solution in PGMEA at 314 rad/s onto silicon wafers. These films were then subject to post-apply bake (PAB) at 110 °C for 60 s. Films of neat PBOCSt and poly(hydroxy styrene) (PHS) were prepared in the same manner with the exception that the PHS samples were post-apply baked at 150 °C for 60 s; these spectra are used for reference.

## NEXAFS

NEXAFS measurements were conducted at the U7A beam line of the National Synchrotron Light Source at Brookhaven National Laboratory. The experimental conditions have been described elsewhere.[5] The spectra were collected with the incident beam at the magic angle $(54.7^{\circ})$ relative to the sample to remove any polarization dependence. For the NEXAFS spectra in this paper the experimental standard uncertainty in the peak position is $\approx \pm 0.15$ eV. The relative uncertainty in the NEXAFS intensity is less than $\pm 5$ % and was determined by multiple scans on a sample. Spectra are collected in a non-destructive manner; this was confirmed by taking multiple scans on a sample and observing no changes in spectral features indicative of chemical changes.

When acquiring NEXAFS spectra, soft X-rays are preferentially absorbed by the sample when the incident radiation is at the appropriate energy to excite a core shell electron to an unoccupied molecular orbital. Auger electrons and photons are emitted when the excited core electron from the irradiated sample relaxes.[6] Electrons emitted from deep within the film cannot escape; only electrons from the near surface of the film (up to 6 nm for carbon *K*-edge electron yield spectra) have enough kinetic energy to escape the surface potential. The electron yield detector has a grid where a negative voltage bias can be applied. Electrons that escape the surface but are emitted from furthest within the film are low in energy due to inelastic interactions with other atoms. These low energy electrons lack enough kinetic energy to pass the detector bias and are not detected. If the negative bias voltage is gradually increased, progressively higher kinetic energy electrons are detected and the effective electron yield sampling depth gets closer to the film surface. All of the electron yield spectra presented below were acquired with a detector bias of -50 V, -150 V, or -200 V and are pre-edge jump normalized (i.e., background subtracted). Photons are emitted from up to ≈200 nm into the film and are detected by a fluorescence yield detector. In order to obtain adequate bulk spectra, the fluorescence yield is measured for four spots on each sample and the collected spectra are averaged.

For the *in situ* environmental stability studies, high purity N-methyl pyrrolidone (NMP) with $\approx 5 \times 10^{-6}$ mole fraction uncyclized amine was prepared by a series of freeze-pump-thaw cycles and admitted to the NEXAFS load chamber through a gas handling system attached to a leak valve. To introduce pure NMP into the load chamber, the gas handling system was purged with NMP and pumped out several times. For all of the experiments involving introduction of contaminant gas to the NEXAFS load chamber, the starting base pressure was $10^{-2}$ Pa or better. For some studies, NMP was combined with the ambient air in the gas handling system before introduction into the load chamber. The vapor pressure of pure NMP at 20 °C (the approximate temperature of the gas handling system) is 40 Pa; therefore, load chamber pressures in excess of 40 Pa are balance ambient atmospheric vapor. Introduction of pure NMP alone gives an approximate amine dose of $2 \times 10^{-9}$ mole fraction (i.e., 2 ppb), comparable to the amount in filtered air used in manufacturing lines. Some *in situ* studies were also performed with degraded NMP (allowed to age in ambient for six months) and water vapor.

## 3. RESULTS AND DISCUSSION

### Segregation in 157 nm blend films
NEXAFS carbon *K*-edge electron yield spectra of neat PNBHFA and P(TBTFMA-NBHFA) and various blend compositions (75:25, 50:50, and 25:75 mass ratio) are shown in Figure 1. Figure 1 also shows the same for the

PNBHFA:P(MCPTFMA-NBHFA) blend system. It has previously been shown that the electron and florescence yield spectra of the neat polymers agree, indicating there are no depth dependent chemical changes in these materials.[7]

The spectra shown in Figure 1 have a prominent C 1s → $\sigma^*_{C-F}$ transition at 295.1 eV corresponding to the C-F bonds in these materials. In the top spectra in Figure 1, the sharp peak at 288.5 eV corresponds to the C 1s → $\pi^*_{C=O}$ transition from the carbonyl of TBTFMA and MCPTFMA, respectively. This provides a signature peak for the copolymers in contrast to the PNBHFA homopolymer, which has no carbonyl moiety. In all of the figures, open symbols correspond to experimental spectra and solid lines represent a linear combination of the component [PNBHFA and P(TBTFMA-NBHFA) or PNBHFA and P(MCPTFMA-NBHFA)] spectra. For all of the blend samples in this study, the fluorescence yield spectra (shown elsewhere)[7] were fit identically with a linear combination of the component spectra corresponding to the bulk compositions. For example, the 50:50 blend film fluorescence yield spectrum was fit with 50 % PNBHFA fluorescence yield spectrum and 50 % P(TBTFMA-NBHFA) fluorescence yield spectrum. The electron yield spectra of the neat polymers shown in Figure 1 provide the component spectra for the linear combination fits of the blend film spectra. For example, the electron yield spectra of the 50:50 PNBHFA:P(MCPTFMA-NBHFA) blend film spectrum shown is fit by a combination of 57 % PNBHFA spectra (bottom) and 43 % P(MCPTFMA-NBHFA) spectra (top). The ratios of component spectra used in the fits are shown in Table I.
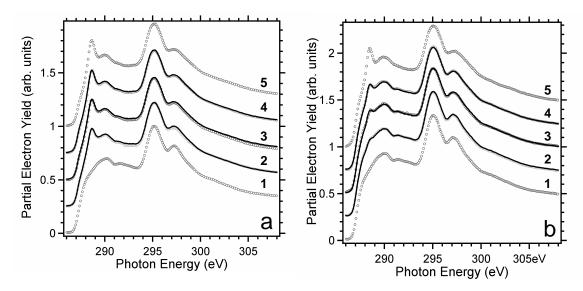


**FIGURE 1.** NEXAFS carbon *K*-edge electron yield spectra of neat and blend samples. Blend ratios are mass fraction PNBHFA: P(TBTFMA-NBHFA) (a) or PNBHFA:P(MCPTFMA-NBHFA) (b). Spectra, bottom to top, are (1) homopolymer, (2) 75:25, (3) 50:50, (4) 25:75, and (5) copolymer. Open symbols correspond to experimental spectra and solid lines represent a linear combination of the component spectra. Spectra are vertically offset for clarity.

Unlike the neat polymers, the blends' surface compositions are different from the bulk and indicate surface segregation. The P(TBTFMA-NBHFA) copolymer segregates to the surface of PNBHFA:P(TBTFMA-NBHFA) blend films (C 1s → $\pi^*_{C=O}$ peak at 288.5 eV enhanced at surface relative to bulk). In contrast, the PNBHFA homopolymer segregates to the surface of the PNBHFA:P(MCPTFMA-NBHFA) blend films, evident by the intensity of the C 1s → $\pi^*_{C=O}$ peak at 288.5 eV, which is diminished at the surface compared to the bulk. Surface segregation of one blend component likely occurs during the spin-coating process due to a slight difference in solvent quality for the blend components. Segregation as a result of the relatively short bake times typical of photoresist processing is less likely because the glass transition temperatures of these polymers are over 150 °C. Residual casting solvent present in the blend films could reduce the effective glass transition temperature, facilitating diffusion within the film during the baking process; however, the residual PGMEA concentration in PNBHFA baked at 130 °C for 60 s is only 0.4 % mass fraction.[8] Also, it is possible that the apparent glass transition temperature will depend on film thickness due to the segregation. For the PNBHFA:P(TBTFMA-NBHFA) blend system, the more hydrophobic copolymer wets the blend film surface as is expected when cast from an organic solvent in air. The interesting point to note is that the PNBHFA homopolymer is more hydrophilic than the P(MCPTFMA-NBHFA) copolymer, therefore, it is expected that the copolymer would wet the blend film surface when spin-coated from an organic solvent and heated in air. These

observations do not agree with hydrophobicity arguments alone as compared to the water contact angle (in degrees) of PNBHFA, P(TBTFMA-NBHFA), and P(MCPTFMA-NBHFA) are 70.6, 87, and 81.6, respectively.[2] This 'inverted' segregation behavior of the PNBHFA:P(MCPTFMA-NBHFA) system may result from differential solubility in the casting solvent. To test this hypothesis, 50:50 blend films of PNBHFA:P(MCPTFMA-NBHFA) were spun cast from cyclohexanone and ethyl lactate on wafers prepared with HMDS (hydrophobic) or native oxide (hydrophilic) surfaces. The result was the same, as shown in Figure 2. The segregation behavior of this blend system is a dramatic departure from what would be expected and provides excellent motivation for further study to elucidate the cause of this surface enrichment of the PNBHFA homopolymer. This result has implications for blend formulation design, regardless of exposure wavelength.

Table I. Compositions of the linear combinations of component spectra used to fit the surface spectra of various blend films. Fits are $\pm\approx5$ %.

| Initial blend composition PNBHFA:P(TBTFMA-NBHFA) | Surface composition P(TBTFMA-NBHFA)* |
|---|---|
| 75:25 | 0.6 |
| 50:50 | 0.8 |
| 25:75 | 0.8 |
| Initial blend composition PNBHFA:P(MCPTFMA-NBHFA) | Surface composition PNBHFA* |
| 75:25 | 0.8 |
| 50:50 | 0.6 |
| 25:75 | 0.5 |

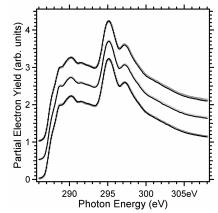*Cast on wafer prepared with native oxide.



**FIGURE 2.** NEXAFS carbon *K*-edge electron yield spectra of PNBHFA:P(MCPTFMA-NBHFA) 50:50 blends. Spectra, bottom to top, are cast from PGMEA, cyclohexanone, and ethyl lactate. Open symbols are on wafers with native oxide, solid lines are on wafers coated with HMDS. Spectra are vertically offset for clarity.

An interesting result of the surface segregating behavior of this blend system is that the PNBHFA homopolymer is not protected and does not undergo a chemical change during deprotection. The PNBHFA homopolymer is soluble in aqueous base developer without modification. Figure 3 shows the resulting spectra from a 50:50 blend films of PNBHFA: P(TBTFMA-NBHFA), left, and PNBHFA:P(MCPTFMA-NBHFA), right, subjected to PAB and developed as described above in a series of TMAH developer concentrations. For the PNBHFA:P(TBTFMA-NBHFA) blend system, no development occurs due to the fact that the protected (and therefore insoluble) copolymer wets the film surface. For the PNBHFA:P(MCPTFMA-NBHFA) system, the developers dissolve away the PNBHFA rich surface layer and the resulting surfaces have compositions closer to that of the bulk materials. The spectra on the left in Figure 3, from the bottom, are 50:50 blend film as cast (PAB only), developed in deionized water, 0.0325 M[‡], 0.065 M, 0.13 M, 0.195 M; and 0.26 M TMAH. All spectra are identical and fit the original blend film surface as described above for this system. The spectra on the right in Figure 3, from the bottom, are: neat PNBHFA; 50:50 blend film as cast (PAB only), developed in deionized water, 0.0325 M, 0.065 M, 0.1 M, 0.18 M TMAH; neat P(MCPTFMA-NBHFA). From the fits, the 50:50 blend films surface compositions of PNBHFA are (from bottom, by mass): 0.68, 0.66, 0.57, 0.63, 0.53, and 0.44.

Although it has been shown that the protected copolymer preferentially wets the surface of the PNBHFA:P(TBTFMA-NBHFA) blend film, the deprotected version of the copolymer has been shown to have a lower water contact angle (59°) than the homopolymer.[2] Consequently, it is expected that partially deprotected P(TBTFMA-NBHFA) will have comparable wetting characteristics and dissolution behavior compared to the PNBHFA homopolymer. However, it is important to further investigate the implications of surface segregation and formation of a wetting layer in these blend film formulations in order to anticipate issues that may arise in the line edge region. For the PNBHFA:P(MCPTFMA-

[‡] The accepted SI unit of concentration, mol/L, has been represented by M in order to conform to the convention of these proceedings.

NBHFA) system, it is possible that the presence of a fast dissolving surface layer may affect the persistence of uniform structures through the film and the overall dissolution behavior.

For the blend films prepared from 3 % and 2 % solutions in PGMEA, the same segregation behavior was observed for both blend systems, indicating that the surface enrichment is independent of total film thickness. For blend films prepared with PAG, segregation of both PAG and the respective blend component to the film surface was observed. These results are significant for ultra-thin film photoresists because for sub-100 nm films of photoresist blend formulations, a substantial fraction of the overall film will have composition and imaging, deprotection, and dissolution behavior considerably different from that of the bulk of the film.
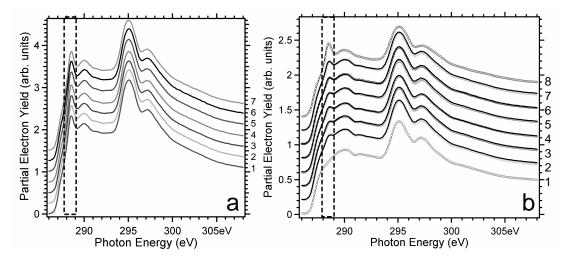


**FIGURE 3.** NEXAFS carbon $K$-edge electron yield spectra of developed 50:50 blend films. a: PNBHFA:P(TBTFMA-NBHFA) (1) as cast (PAB only), (2) developed in deionized water, (3) 0.0325 M, (4) 0.065 M, (5) 0.13 M, (6) 0.195 M, and (7) 0.26 M TMAH. b: (1) neat PNBHFA as cast (PAB only); 50:50 PNBHFA: P(MCPTFMA-NBHFA) blend film (2) as cast (PAB only), (3) developed in deionized water, (4) 0.0325 M, (5) 0.065 M, (6) 0.1 M, (7) 0.18 M TMAH; (8) neat P(MCPTFMA-NBHFA). From the fits of the PNBHFA:P(MCPTFMA-NBHFA) system, the blend films' surface compositions of PNBHFA are (from bottom): 0.68, 0.66, 0.57, 0.63, 0.53, and 0.44. Spectra are vertically offset for clarity. Peak of interest (288.5 eV corresponding to C 1s → $\pi^*_{C=O}$ transition from copolymer) highlighted in dashed box.

**248 nm environmental stability: *in situ* processing**

The environmental stability of a model photoresist in the presence of airborne molecular contaminants was studied in the NEXAFS line equipped with *in situ* processing capabilities so that ultraviolet exposure, contaminant dosing, and post-exposure bake can be performed to mimic photoresist processing conditions and post-exposure delay. All of the spectra shown in this section are pre- and post-edge jump normalized. Post-edge normalization eliminates the spectral dependence on total carbon content; therefore, changes in the NEXAFS spectra are indicative of changes in chemical functionality. NEXAFS is a well-suited technique to probe the deprotection reaction for the PBOCSt/PFOS system because the C=O peak unique to PBOCSt is indicative of the protected fraction. Figure 4 shows NEXAFS carbon $K$-edge electron yield spectra from films of (a) (from bottom) PBOCSt with PFOS, neat PBOCSt, and neat PHS, and (b) PBOCSt with PFOS films at different detector biases (i.e., different depths into the film surface). For each of the spectra, the first peak at 285.0 eV corresponds to the C 1s → $\pi^*_{C=C}$ transition from the styrene ring. Splitting of the $\pi^*_{C=C}$ resonance in PHS is visible at ≈ 287.5 eV. As demonstrated in Figure 4a, PBOCSt is easily distinguished from PHS, its deprotected counterpart. For PBOCSt, the carbonyl C 1s → $\pi^*_{C=O}$ transition is reflected in the peak at 290.3 eV; this peak is absent from the PHS spectra. Because of the loss of $CO_2$ (resulting in diminished $\pi^*_{C=O}$ peak) during deprotection of PBOCSt to form PHS, it is possible to fit the extent of deprotection using linear combinations of component spectra (i.e., PBOCSt and PHS). Also shown in Figure 4a is a comparison of neat PBOCSt to the PFOS containing samples used in this study. From the spectral features at 292 eV and 295 eV indicative of C-F bonds it is clear that there is segregation of PFOS to the surface of the prepared films. This result is further illustrated by Figure 4b, showing the PBOCSt/PFOS film surface at multiple detector biases. As the sampling depth moves closer to the surface,

the PFOS concentration increases and is close to 50 % at ≈3.5 nm into the surface. PFOS segregation has been previously reported for this system.[5] For all of the results shown in the remaining figures, the detector bias is -150 V.
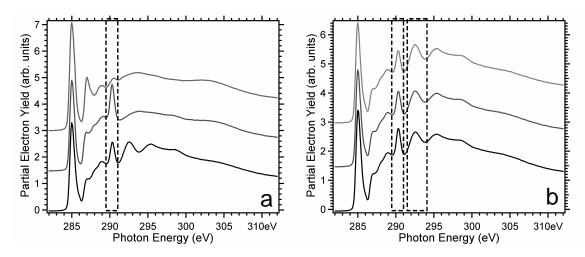


**FIGURE 4.** NEXAFS carbon $K$-edge electron yield spectra. Descriptions of spectra are in order from bottom to top. (a) Reference samples following PAB (PBOCSt with PFOS, PBOCSt, and PHS, all at -150 V detector bias), showing significant segregation of PFOS to the surface of the sample films and the spectral differences between PBOCSt and PHS. (b) PBOCSt with PFOS shown at variable detector bias (-50 V, -150 V, and -200 V), indicating that the concentration of PFOS increases closer to the film surface (compare relative peak intensities at 290.3 eV and 292 eV). Spectra are vertically offset for clarity. All spectra are pre- and post-edge normalized to remove dependence on total carbon content.

In order to assess the feasibility of processing the PBOCSt/PFOS samples in the ultra-high (UHV) vacuum conditions required for NEXAFS analysis (typical analysis chamber pressure $10^{-6}$ Pa, slightly higher pressure in load chamber), a single sample was subjected to 90 mJ/cm$^2$ ultra-violet (UV) exposure from a broadband source (peak intensity 254 nm) then post-exposure baked at 90 °C for increasing time increments. The sample stage is introduced to the chamber at room temperature and not heated during UV exposure or analysis; therefore, the sample holder temperature is actually ramped to the desired temperature within 3 min. Because of the controlled environment of the UHV chamber, we do not expect this delay to affect the chemistry of the deprotection reaction in the absence of deliberately introduced airborne molecular contaminants. Spectra were collected between heating steps to monitor the progression of deprotection. The result is shown in Figure 5a. From the bottom, the spectra are PBOCSt with PFOS (1) PAB only, (2) UV exposed with temperature heated to 90 °C and held for 5 s, (3) heated to 90 °C and held 4 min, (4) heated again at 90 °C for additional 4 min (total 8 min), and (5) neat PHS, for comparison. By following the intensity of the C=O peak at 290.3 eV it is evident that the deprotection increases with increased heating, with the sample being ≈60 % protected after the first brief heating increment, almost completely deprotected after 4 min, and completely deprotected after a total of 8 min of heating. It is important to note that the C-F peaks at 292 eV and 295 eV indicative of PFOS presence at the surface decrease with increased heating and are totally absent in the completely deprotected sample. PFOS in its salt form before exposure does not sublime from the surface of the film during heating. The C-F peak intensity reduction could be explained by diffusion of PFOS from the surface into the bulk of the photoresist film due to better mixing with PHS or sublimation of the photogenerated acid.[5]
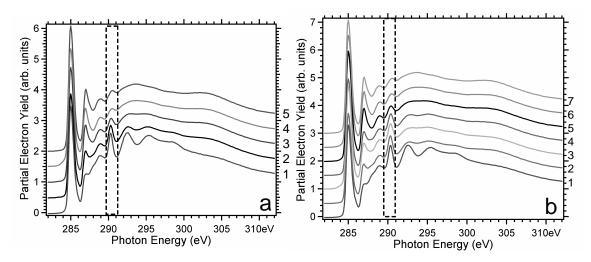
**FIGURE 5**. NEXAFS carbon *K*-edge electron yield spectra. Descriptions of spectra are in order from bottom to top. All spectra were taken at -150 V detector bias and are PBOCSt/PFOS films unless otherwise noted. (a) Monitoring the extent of deprotection during *in situ* processing of one sample, (1) PAB only, (2) UV exposed with temperature ramped to 90 °C and held for 5 s, (3) heated to 90 °C and held 4 min, (4) heated again to 90 °C and held for additional 4 min (total 8 min at 90 °C, 15 min total at elevated temperature), and (5) neat PHS, for comparison. (b) Monitoring deprotection inhibition with introduction of NMP, (1) PAB only, (2) 60 mJ/cm$^2$ UV exposure followed by PEB at 90 °C for 8 min in the presence of 205.3 Pa NMP and ambient ($\approx$70 % protected), (3) 60 mJ/cm$^2$ UV exposure followed by PEB at 90 °C for 8 min in the presence of 70.7 Pa NMP and ambient ($\approx$50 % protected), (4) 60 mJ/cm$^2$ UV exposure followed by PEB at 90 °C for 8 min in vacuum ($\approx$50 % protected), (5) 60 mJ/cm$^2$ UV exposure followed by 60 s delay, then PEB at 90 °C for 8 min in the presence of 0.4 Pa NMP, (6) 60 mJ/cm$^2$ UV exposure followed by 1.25 h delay, then PEB at 90 °C for 8 min in vacuum, and (7) neat PHS, for comparison. Spectra are vertically offset for clarity. All spectra are pre- and post-edge normalized to remove dependence on total carbon content.

As an additional check of the *in situ* processing, an identical sample was subjected to 60 mJ/cm$^2$ UV exposure and 8 min of heating at 90 °C to achieve partial deprotection, then similarly exposed and baked again and was completely deprotected. The same loss of PFOS C-F peaks from the surface was observed.

Confident that we are able to mimic typical photoresist processing with the *in situ* system, it is now necessary to confirm that failure caused by PED is a result of airborne molecular contaminants and not a result of the intrinsic chemistry of the system. Once this was confirmed, a model airborne molecular contaminant, NMP, was introduced into the chamber during UV exposure and post-exposure bake to simulate the effect of post-exposure delay (PED) during normal photoresist processing. A selection of the results are shown in Figure 5b; from bottom to top: (1) initial PBOCSt/PFOS sample with PAB only, (2) 60 mJ/cm$^2$ UV exposure followed by PEB at 90 °C for 8 min in the presence of 205.3 Pa NMP and ambient ($\approx$70 % protected), (3) 60 mJ/cm$^2$ UV exposure followed by PEB at 90 °C for 8 min in the presence of 70.7 Pa NMP and ambient ($\approx$50 % protected), (4) 60 mJ/cm$^2$ UV exposure followed by PEB at 90 °C for 8 min in vacuum ($\approx$50 % protected), (5) 60 mJ/cm$^2$ UV exposure followed by 60 s delay, then PEB at 90 °C for 8 min in the presence of 0.4 Pa NMP, (6) 60 mJ/cm$^2$ UV exposure followed by 1.25 h delay, then PEB at 90 °C for 8 min in vacuum, and (7) neat PHS, for comparison. The comparability of spectra (3) and (4) in Figure 5b is expected because such low levels of contaminant should not affect the deprotection of the photoresist. However, having a higher pressure of ambient in the chamber with the NMP caused inhibition of the deprotection reaction, as shown in spectrum (2) of the same figure. This result was confirmed by similar processing of identical samples and inhibition was always enhanced with the presence of ambient air with NMP. Spectra (5) and (6) of Figure 5b demonstrate that airborne molecular contaminants are the cause of deprotection inhibition during PED; the sample shown in spectrum (6) was left for a PED of 1.25 h in UHV and deprotected completely [compare to PHS, spectrum (7)]. The sample shown in spectrum (5) was given a PED of only 1 minute in very low concentration of NMP and was almost completely deprotected. It appears as though PED in a controlled environment has the ability to enhance deprotection; studies are ongoing to investigate this further. This result is also shown below in Figure 6c, top spectrum.
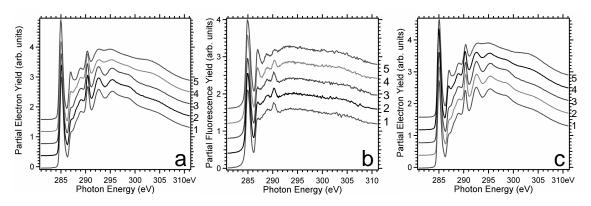
**FIGURE 6**. NEXAFS carbon *K*-edge electron (left, right) and fluorescence (center) yield spectra. Descriptions of spectra are in order from bottom to top. All electron yield spectra were taken at -150 V detector bias. All samples are PBOCSt/PFOS films. (a) Monitoring surface deprotection during *in situ* processing for different levels of contamination with degraded NMP. All samples in this plot were subjected to UV exposure (90 mJ/cm$^2$) and PEB (90 °C for 8 min). (1) 26.7 Pa, (2) 13.3 Pa, (3) 6.7 Pa, (4) 1.3 Pa, and (5) no NMP. (b) Fluorescence yield (bulk) for the same samples described in a. (c) Monitoring surface deprotection (1) PAB only, (2) 60 mJ/cm$^2$ UV exposure followed by PEB at 90 °C for 5 min in 26.7 Pa degraded NMP, (3) 60 mJ/cm$^2$ UV exposure followed by PEB at 90 °C for 5 min in the presence of 1466 Pa water vapor, (4) 60 mJ/cm$^2$ UV exposure followed by PEB at 90 °C for 5 min in vacuum, (5) 60 mJ/cm$^2$ UV exposure followed by 12 min delay, then PEB at 90 °C for 5 min in vacuum. Spectra are vertically offset for clarity. All spectra are pre- and post-edge normalized to remove dependence on total carbon content.

From the studies described above, it is shown that deprotection inhibition is worse when ambient atmosphere is allowed to enter the NEXAFS chamber with pure NMP. Ambient atmosphere has some amount of water vapor which may enhance inhibition. In order to test this hypothesis, studies were performed with both degraded NMP and water vapor to monitor the deprotection inhibition. Figure 6 shows that inhibition of surface deprotection is augmented with the use of degraded NMP (expected to have both a greater concentration of uncyclized amines and water vapor) and that water vapor alone is enough to inhibit deprotection. Also shown is the bulk data for various concentrations of degraded NMP contamination; the bulk data correspond to the surface data indicating that the inhibition occurs not only at the surface, but also in the bulk, although to a lesser extent. Figure 6a and 6b show that as the concentration of degraded NMP introduced into the chamber was reduced from 26.7 Pa to 6.7 Pa, the extent of deprotection was relatively constant, while at 1.3 Pa degraded NMP, the extent of deprotection increased. This implies that there is a contamination threshold for these materials, above which the level of inhibition remains consistent with airborne molecular contaminant concentration and below which inhibition is reduced. Figure 6c shows that water vapor can inhibit to the same degree as high levels of basic contaminant. This water vapor contamination effect has previously been observed.[9] Considering this effect of water vapor, it is possible that current schemes to reduce the concentration of amines present during wafer processing are inadequate to address the environmental stability issue, particularly for 157 nm photoresists, which are known to be more environmentally sensitive.

## 4. CONCLUSIONS

The newest generation of photoresists, including thin film 157 nm fluorinated copolymers and blends, present a number of materials' issues, including polymer/substrate and polymer/air interfacial (surface energy) effects, blend miscibility, and small molecule diffusion in thin films. The chemical composition of the surface and bulk chemistry of various blend compositions of model 157 nm photoresists were investigated with NEXAFS to quantify component segregation and identify surface phenomena that may be responsible for pattern degradation. It was found that there is segregation of one component to the surface of the photoresist film, in excess of the composition of that component in the blend. This information suggests that substantial surface effects related to the relative surface energy of the constituent polymers and other additives occur in these blend formulations. As photoresist film thickness continually decreases and the interfacial regions dominate the behavior of the material, it is crucial to understand both their physical and chemical nature.

NEXAFS is a powerful tool for measuring the depth dependent surface chemistry in model chemically amplified photoresists. The capability to measure both PAG segregation and PED effects on the surface chemistry are important contributions to the understanding of photoresist performance. It has been shown that photoresist films are very sensitive to certain airborne contaminants, notably amines, during post-exposure delay, though the actual cause and

specific failure mechanism are unknown. In order to better understand the effect of low concentrations of atmospheric species on the performance of chemically amplified photoresists and possible failure mechanisms, an environmentally controlled system has been developed that allows fine tuning of processing conditions coupled with immediate surface characterization using near edge x-ray absorption fine structure spectroscopy (NEXAFS). The surface chemistry of model photoresists was analyzed using NEXAFS equipped with *in situ* processing capabilities for exposure, controlled dosing of a model contaminant gas, and heating to quantify component segregation and identify surface phenomena that may be responsible for pattern degradation. It has been found that photo-acid generator segregates to the surface of the photoresist film; as film thickness becomes progressively thinner and the chemistry of the photoresists changes as more fluorinated components are incorporated, the behavior of this PAG-rich, high fluorine content surface layer may introduce additional/unique sensitivity to airborne contaminants and failure mechanisms compared to previous photoresist materials. This technique is therefore valuable to elucidate the influence of atmospheric contaminants in chemically amplified photoresists, particularly with the move toward new chemistries and thinner films, which have been shown to be more environmentally unstable compared to past materials.

## ACKNOWLEDGMENTS

## REFERENCES

[1] http://public.itrs.net/

[2] H. Ito, G. M. Wallraff, N. Fender, P. J. Brock, W. D. Hinsberg, A. Mahorowala, C. E. Larson, H. D. Truong, G. Breyta, and R. D. Allen, J. Vac. Sci. Technol. B 19, 2678 (2001) and H. Ito, H. D. Truong, M. Okazaki, D. C. Miller, N. Fendler, P. J. Brock, G. M. Wallraff, C. E. Larson, and R. D. Allen, J. Photopolym. Sci. Technol. B 15, 591 (2002).

[3] S. A. MacDonald, W. D. Hinsberg, H. R. Wendt, N. J. Clecak, and C. G. Willson, Chem. Mater. 5, 348 (1993).

[4] W. D. Hinsberg, S. A. MacDonald, and N. J. Clecak, Chem. Mater. 6, 481 (1994).

[5] J. L. Lenhart, R. L. Jones, E. K. Lin, C. L. Soles, W.-l. Wu, D. A. Fischer, S. Sambasivan, D. L. Goldfarb, and M. Angelopolous, J. Vac. Sci, Technol. B 20, 2920 (2002).

[6] J. Stohr, *NEXAFS Spectroscopy*, Springer-Verlag: Berlin Heidelberg, 1992.

[7] E. L. Jablonski, V. M. Prabhu, S. Sambasivan, E. K. Lin, D. A. Fischer, D. L. Goldfarb, M. Angelopoulos, and H. Ito, J. Vac. Sci. Technol. B 21, 3162 (2003).

[8] H. Ito, H. D. Truong, M. Okazaki, D. C. Miller, N. Fender, G. Breyta, P. J. Brock, G. M. Wallraff, C. E. Larson, and R. D. Allen, Proc. SPIE 4690, 18 (2002).

[9] J. Nakamura, H. Ban, Y. Kawai, and Al Tanaka, J. Photopolym. Sci. Technol. B 8, 555 (1995).